Diagnostics of Hall Thruster Plume by Laser Absorption Spectroscopy

Shigeru Yokota[*], Makoto Matsui[†], Daichi Sako[‡]
The University of Tokyo, Tokyo, 113-8656, JAPAN

Naoji Yamamoto[§]
Kyushu University, Tokyo, 816-8580, JAPAN

Hiroyuki Koizumi[**], Kimiya Komurasaki[††]
The University of Tokyo, Tokyo, 133-8656, JAPAN

Hideki Nakashima[‡‡]
Kyushu University, Fukuoka, 816-8580, JAPAN

and

Yoshihiro Arakawa[§§]
The University of Tokyo, Tokyo, 113-8656, JAPAN

Plume characteristics of a magnetic layer type Hall thruster were evaluated by laser absorption spectroscopy and single probe measurement. Translational temperature and total number density distributions of xenon atom were deduced using an absorption line of XeI 823.16 nm and electron temperature. As a result, the temperature was around 430±50 K in the almost all measured region, which agreed with the thermocouple measurement though it might be overestimated 850 K at the channel exit due to the Zeeman effect. The maximum total number density was 3.9×10^{19} m^{-3} at the channel exit. Then, the number density decreased by one order at 200 mm away from the exit.

Nomenclature

A	=	Einstein coefficient, s^{-1}
g	=	statistical weight
h	=	Planck's constant, J.s
I	=	probe laser intensity, mW/mm^2
I_0	=	incident laser intensity, mW/mm^2
k	=	absorption coefficient, m^{-1}
k_B	=	Boltzmann constant, J/K
K	=	integrated absorption coefficient, GHz m^{-1}
M	=	atomic mass, kg
n	=	number density, m^{-3}
r	=	radial coordinate, mm

[*] Graduate student, Department of Aeronautics and Astronautics, Student Member AIAA.
[†] JSPS Research Fellow, Department of Aeronautics and Astronautics, matsui@al.t.u-tokyo.ac.jp. Member AIAA.
[‡] Graduate student, Department of Aeronautics and Astronautics.
[§] Research Associate, Department of Advanced Energy Engineering Science, Member AIAA.
[**] Research Associate, Department of Aeronautics and Astronautics, Member AIAA.
[††] Associate Professor, Department of Advanced Energy, Member AIAA.
[‡‡] Professor, Department of Advanced Energy Engineering Science, Member AIAA.
[§§] Professor, Department of Aeronautics and Astronautics, Member AIAA.

R = plume radius, mm
T = translational temperature, K
T_e = electron temperature, eV
x = coordinate in the laser pass direction, mm
y = probe beam position, mm
z = axial coordinate, mm
α^A = natural abundance of xenon
$\beta^A_{Fi,\,Fj}$ = relative intensity of nuclear spitted line
$\gamma^A_{Fi,Fj}$ = correction coefficient of Doppler width
ΔE = energy gap, eV
λ = wavelength, nm
ν = laser frequency, Hz
ν_0 = center absorption frequency, Hz
$\nu^A_{0,\,IS}$ = isotope shift of center absorption frequency, GHz
$\nu^A_{0,\,Fi,\,Fj}$ = nuclear spin shift of center absorption frequency, GHz
$\Delta\nu_D$ = Doppler width, GHz

Subscript
i = absorption state
j = excited state
tot = total states

Superscript
A = atomic mass, amu

I. Introduction

Hall thrusters are one of the promising thrusters of satellites for orbit transfer or North/South station keeping missions because it produces high thrust efficiency, exceeding 50%, with a specific impulse range of 1000-3000 s and a higher ion beam density than ion thrusters because of the existence of electrons in the ion acceleration zone. This is because a moderate magnetic field is applied in the acceleration zone, causing the magnetization of the electrons and not the ions.[1-3]. Hence, several types of Hall thrusters are actively developed in Russia, USA, EU and Japan[4-10].

In their practical use in a spacecraft, the interactions between the plume of the thruster and the host spacecraft cause serious problems[11-13]. High-energy main beam ions generated and accelerated in the acceleration channel collide with unionized propellant atoms in the plume, resulting in the production of low-energy ions and high-energy atoms by charge exchange reaction (CEX). These CEX ions propagate in the radial and upstream directions because of the potential distribution near the spacecraft. The backflow of CEX ions becomes a contamination source causing erosion, sputtering, degradation, increment of temperature and potential change of solar arrays or spacecraft surfaces.

Recently, a plume shield has been developed to protect the spacecraft from CEX ions. The plume shield developed by Mitsubishi Electric Corporation intercepts ions with higher angle beyond 45 degree[14]. Then, it is important to clarify a production mechanism of CEX reactions to evaluate the shields performances and optimization. Plume characteristics have been a hot subject and investigated experimentally in ground-based facilities[15-20] and even in an actual flight test[21] as well as numerical calculations[22-25]. Because most of measurements, however, are conducted by intrusive probe methods such as electrostatic probes, energy analyzers and mass spectrometers, measurements near the thruster exit are difficult for their disturbances, where CEX reactions would most frequently take place[14-20]. The plume properties near the thruster exit are also useful for initial conditions of numerical calculations.

In this study, laser absorption spectroscopy (LAS) and single probe measurement were applied to a magnetic-layer-type Hall thruster plume developed at the University of Tokyo[9]. Number density and temperature distributions of neutral xenon atom are deduced from measured absorption profiles at 823.16nm ($6s[3/2]^0_2 \rightarrow 6p[3/2]_2$) and the electron temperature assuming Boltzmann equilibrium among all excited states.

II. Theory of Laser Absorption Spectroscopy

Laser absorption spectroscopy has some superiority to other non-intrusive spectroscopes such as emission and LIF: 1) it is applicable to optically thick plasma, and 2) absolute calibration using a standard light source or a density reference cell is not necessary. Moreover, 3) the measurement system is portable when a diode laser is used[26].

A. Absorption Coefficient and Number Density

The relationship between probe laser intensity I and absorption coefficient $k(x)$ is expressed by the Beer-Lambert law as[27],

$$\frac{\mathrm{d}I}{\mathrm{d}x} = -k(x)I\,. \tag{1}$$

Because distributions of absorption properties in plumes would be axisymmetric, local absorption coefficient $k_\nu(r)$ with the radial coordinate r is obtained by the Abel inversion expressed as[28],

$$k(r) = \frac{1}{\pi}\int_r^R \frac{d(\ln\frac{I}{I_0}(y))}{dy}\frac{dy}{\sqrt{y^2-r^2}}\,. \tag{2}$$

Assuming Boltzmann relation between absorbing and excited states, integrated absorption coefficient $K(r)$ is expressed as a function of the number density at the absorbing state $n_i(r)$ as[27],

$$K(r) = \int_{-\infty}^{\infty} k_\nu(r)\mathrm{d}\nu = \frac{\lambda^2}{8\pi}\frac{g_j}{g_i}A_{ji}n_i(r)\left[1-\exp\left(-\frac{\Delta E_{ij}}{k_\mathrm{B}T_\mathrm{e}}\right)\right]. \tag{3}$$

Assuming Boltzmann relations among all excited states, total number density n_{tot} is deduced from measured number density as,

$$n_{\mathrm{tot}} = \frac{n_i}{g_i}\sum_l g_l \exp\left(-\frac{\Delta E_{li}}{k_\mathrm{B}T_\mathrm{e}}\right). \tag{4}$$

Here summation l is taken for all states[29].

B. Line broadening and Translational Temperature

An absorption profile of an atomic line is broadened by various physical mechanisms, and then expressed by a convolution of the Lorentz and the Gauss distributions. However, in low-pressure plasma, Doppler broadening is dominant and the other broadenings such as natural, pressure, Stark broadenings are negligible[26]. Then, in this study, only Doppler broadening is considered.

The proper frequency ν_0 of a moving atom at velocity v is observed to be shifted by the Doppler effect resulting in causing broadening of the profile. This is called the Doppler broadening. This broadening is the Gauss distribution and its full width at half maximum (FWHM) $\Delta\nu_\mathrm{D}$ is related to the translational temperature T as[27],

$$\Delta\nu_D = \frac{2\nu_0\sqrt{\ln 2}}{c}\sqrt{\frac{2k_\mathrm{B}T}{M}}\,. \tag{5}$$

Here, c and M_A are velocity of light and atomic mass.

C. Absorption Profile

Because xenon has nine isotopes and non-zero nuclear spin, its line has a hyperfine structure[30]. Considering the Doppler dominant broadening and the hyperfine structure, the absorption profile is a superposition of twenty-one

Gaussian functions whose relative square are determined by natural abundance and relative intensity of the hyperfine structure. Then, the profile is expressed as,

$$k(\nu) = K \sum_{A,F}^{21} \frac{2\alpha^{A} \beta^{A}_{F_i,F_j}}{\gamma^{A}_{F_i,F_j} \Delta\nu_D} \sqrt{\frac{\ln 2}{\pi}} \exp\left[-\ln 2 \left\{ \frac{2\left(\nu - \nu_0 - \nu^{A}_{0,\mathrm{IS}} - \nu^{A}_{0,F_i,F_j}\right)}{\gamma^{A}_{F_i,F_j} \Delta\nu_D} \right\}^2 \right]. \tag{6}$$

Here, $\gamma^{A}_{Fi,Fj}$ is the correction coefficient of Doppler width. Assuming that translational temperature is independent of the isotopes, Doppler width of each isotope is slightly different from each other due to the difference of mass and center frequency in Eq.(5). Then, $\gamma^{A}_{Fi,Fj}$ is expressed as,

$$\gamma^{A}_{F_i,F_j} = \frac{\nu_0^{132} + \nu^{A}_{0,\mathrm{IS}} + \nu^{A}_{0,F_i,F_j}}{\nu_0^{132}} \sqrt{\frac{M_{132}}{M_A}}. \tag{7}$$

Here, the natural abundance, isotope shift, and nuclear spin shift were referred in Ref. 31-34.

III. Experimental Setup

A. Magnetic-layer-type Hall thruster

Figures 1 and 2 show a cross section of a magnetic-layer-type Hall thruster and its photo in operation. The inner and outer diameters of the acceleration channel are 48 and 62 mm, respectively. An acceleration channel wall was made of BN. The anode is located at 21 mm, upstream end of the acceleration channel. A solenoid coil is set at the center of the thruster to apply a radial magnetic field in the acceleration channel. The magnetic flux density is varied by changing the coil current. There is no outer coil because a uniform magnetic field distribution is maintained along the azimuthal direction. A hollow cathode (7HCN-001-001; Veeco-Ion Tech Inc.) was used as an electron source and a neutralizer. A vacuum chamber of 2 m diameter by 3 m length was used in the experiments. The pumping system comprised a diffusion pump (37000 l/s), a mechanical booster pump (2800 l /s), and two rotary pumps (250 l /s). An operation condition is tabulated in Table 1.

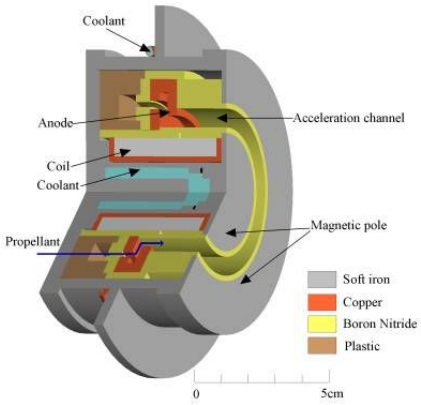

Fig. 1 Cross section of a magnetic layer type Hall thruster.

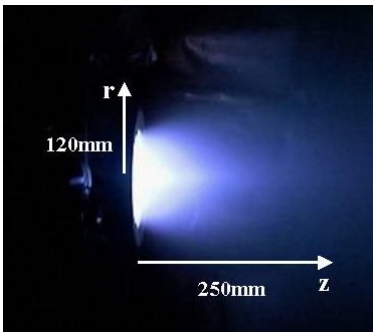

Fig. 2 A photo of a Hall thruster plume.

Table 1 Operation conditions.

Parameter	Value
Working gas	Xenon
Mass flow rate	1.0 Aeq (1.36 mg/s)
Discharge voltage	260 V
Discharge current	1.0 A
Applied magnetic field	0.014 T
Ambient pressure	7.8×10^{-3} Pa

B. Measurement System

Figure 3 shows a schematic of the measurement system. A single longitudinal mode diode-laser (HL8325G; HITACHI Ltd., LDC205; Thorlabs Inc.) was used as the laser oscillator. The laser frequency monitored by a

spectrometer (PMA50; Hamamatsu Photonics K.K.) was roughly matched to the absorption one by temperature control (TED200; Thorlabs Inc.). Then, it was scanned over the absorption line shape by current modulation with a function generator. The modulation frequency and width were 1 Hz and 30 GHz, respectively. An etalon was used as a fine wave-meter. Its free spectral range was 1 GHz.

The probe beam was guided into the vacuum chamber through a multimode optical fiber. The fiber output was mounted on a two-dimensional traverse stage to scan the plume in the radial and axial direction. The spatial resolution determined by the photo detector area was 1 mm. To reduce plasma emission, a band pass filter, whose FWHM was 10 nm, was used. As a reference, absorption signal in glow discharge plasma was also monitored. Its input power, discharge voltage and ambient pressure were 1.5 mW, 500 V, and xenon 79 Pa, respectively. All signals were recorded using a digital oscilloscope (DL708; Yokogawa Co.) with 10-bit resolution.

Measurement range is r<120 mm and z<250 mm as shown in Fig.3. Here, r and z are the radial and axial coordinates.

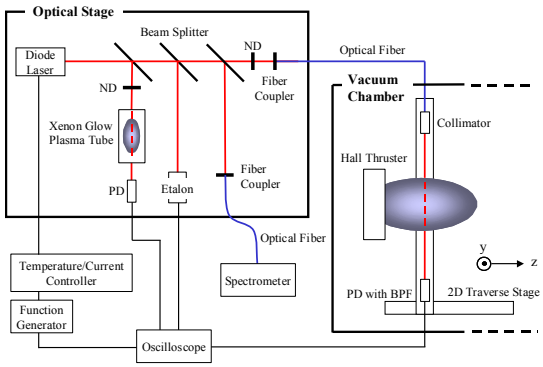

Fig. 3 Measurement system.

IV. Results and Discussion

A. Data Processing

Figure 4 shows transmitted laser intensity signals of the plume and glow plasma and an etalon signal. At each measurement point, eight profiles were recorded. Absorbance was obtained from normalization of the frequency and the transmitted laser intensity by the etalon signal and the laser intensity without absorption. Then, local absorption profiles were reconstructed by the Abel inversion of the absorbance at every 0.05 GHz. Figure 5 shows an absorption profile at z=50 mm, r=20 mm and relative intensity of the hyperfine structure as a bar graph. The peaks of the hyperfine structure were observed at estimated position in frequency. Figure 6 also shows a curve fitting of Eq.(6). The fitting was well on the measured profile. This shows the validation of Gaussian dominant assumption.

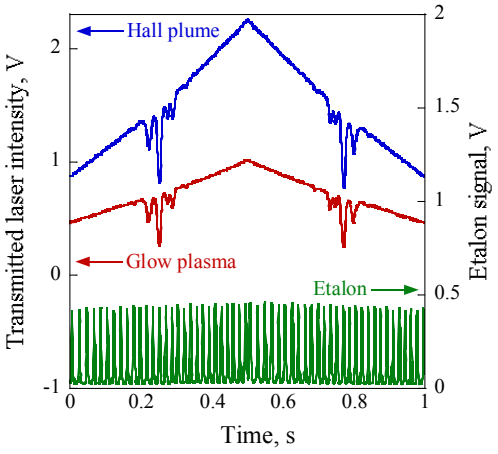

Fig. 4 Transmitted laser intensity signals of Hall plume and glow plasma and etalon signal.

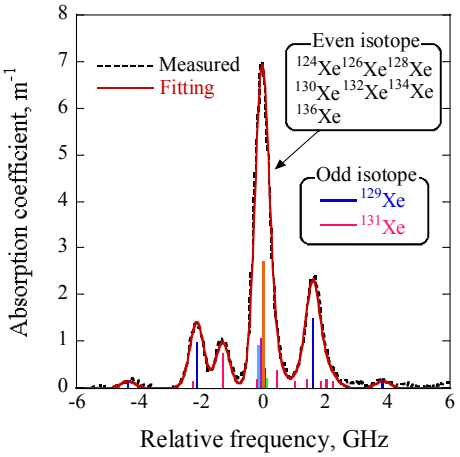

Fig. 5 Absorption profile after Abel inversion and curve fitting. (r=20mm, z=50mm)

B. Temperature Distribution

Figure 6 shows a translational temperature distribution of xenon atom. Here, the error for eight profiles was about 50 K. At the channel exit, the temperature was 850 K, whereas it was around 430 K in other region. However, this higher temperature at the exit might be overestimated because of the Zeeman effect.

To evaluate this result, firstly, the temperature at the edge of the thruster was measured by a thermo-coupler. Figure 7 shows a cross sectional view of the thruster and the measured point. The measured temperature was 393 K. Next, the plasma temperature was estimated by the finite element analysis software (Quickfield 5.0, Tera Analysis Ltd.). Here, the plasma temperature was assumed to be that of the ceramic wall, and the temperature at the edge of the thruster and the cooling water were fixed to 393 K and 293 K, respectively. Figure 7 also shows the calculated temperature distribution. The calculated plasma temperature was 415 K. This value shows a good agreement with the LAS result of 430±50 K.

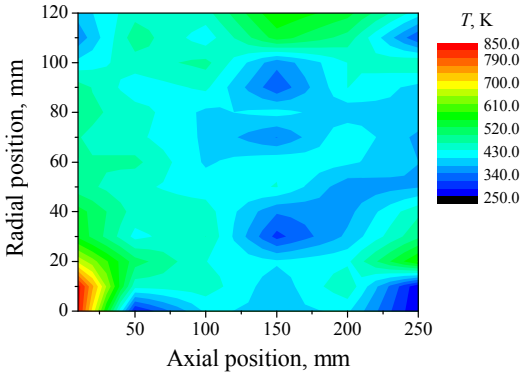

Fig. 6 Temperature distribution by LAS.

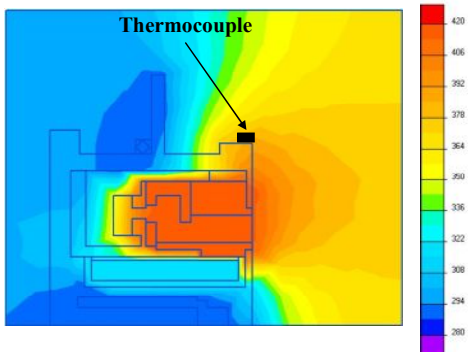

Fig. 7 Temperature distribution by calculation.

C. Number Density Distribution

The electron temperature was measured by a single probe method to deduce the total number density of xenon atom. As a probe, tungsten wire was used; whose diameter and length exposed to the plasma were 0.25 mm and 3 mm, respectively. The applied voltage to the probe was varied from -70 V to 150 V. Figure 8 shows a measured electron temperature distribution. The maximum electron temperature was 7.5 eV near the anode exit and that in the other region was found around 3 to 4 eV.

The total number density distribution of xenon atom was deduced from the measured meta-stable one using Eq. (4). Figure 9 shows deduced total number density distribution. The maximum density is $3.9 \times 10^{19} m^{-3}$ at the channel exit. Then, the number density decreases by one-order at z=200 mm.

The number density estimated from mass flow rate, propellant utilization efficiency of 0.8 and channel exit area of 12.1 cm^2 is 1.2×10^{19} m^{-3} at the channel exit. Here thermal velocity of xenon atom deduced from the measured translational temperature is used. The higher estimation of a factor of four would be originated from higher population of meta-stable than Boltzmann equilibrium.

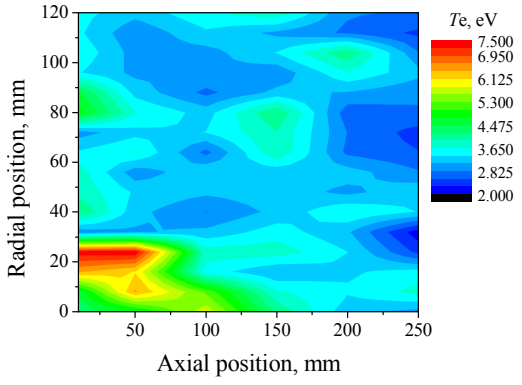

Fig. 8 Electron temperature distribution.

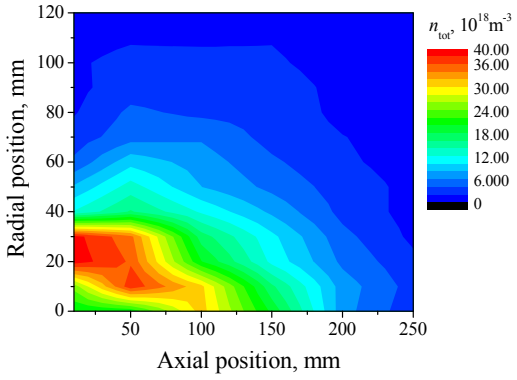

Fig. 9 Number density distribution of xenon atom.

V. Conclusion

Laser absorption spectroscopy was applied to a magnetic layer type Hall thruster plume using an absorption profile of XeI 823.16 nm. The measured profiles after the Abel inversion were fitted by twenty-one Gauss functions considering the isotope shifts and the nuclear spin splitting. The deduced translational temperature was around 430 $\pm$50 K in the almost all measured region, though it might be overestimated 850 K at the channel exit due to the Zeeman effect. This result shows a good agreement with that estimated from the thermo-couple measurement and the finite element analysis. The total number density was estimated from measured meta-stable number density by LAS and electron temperature by the single probe, assuming the Boltzmann equilibrium between meta-stable and the other states. As a result, the maximum number density was 3.9×10^{19} m^{-3} at the channel exit. This value is a factor of four higher than that estimated from the mass flow rate and the propellant utilization efficiency. The number density decreased by one order at 200 mm away from the exit.

Acknowledgments

This work was partially supported by a Grand-in-Aid for Scientific Research (S), No.16106012 and for Research Fellowships of the Japan Society for the Promotion of Science for Young Scientists, 18-09885, 2006 sponsored by the Ministry of Education, Culture, Sports, Science and Technology in Japan

References

[1]Bober A., Maslennikov, N., Day, M., Popov, G. and Rylov, Yu., "Development and Application of Electric Propulsion Thruster in Russia," Proceedings of the 23rd International Electric Propulsion Conference, IEPC 93-001, 1993.

[2]Saccoccia, G., "Introduction to the European Activities in Electric Propulsion," Proceedings of the 28th International Electric Propulsion Conference, IEPC 03-341, 2003.

[3]Blandino, J., "The Year in Review, Electric Propulsion," Aerospace America, Dec. 2003, pp. 60, 61.

[4]Kim, V., "Main Physical Features and Processes Determining the Performance of Stationary Plasma Thrusters," Journal of Propulsion and Power, Vol. 14, No. 5, 1998, pp. 736–743.

[5]Kaufman, H. R., "Technology of Closed-Drift Thrusters," *AIAA Journal*, Vol. 23, No. 1, 1985, pp. 78–86.

[6]Choueiri, E.Y., "Fundamental Difference Between the Two Hall Thruster Variants," *Physics of Plasmas*, Vol. 8, No. 11, 2001, pp. 5025–5033.

[7]Haas, J. M., Gulczinski, F. S., Gallimore, A> D., Spanjers, G. G., and Spores, R. D., "Performance Characteristics of a 5 kW Laboratory Hall Thruster," AIAA Paper 98-3503, 1998.

[8]Valentian, D., and Maslennikov, N., "The PPS 1350 Probram," Proceedings of the 25th International Electric Propulsion Conference, IEPC 97-134, 1997.

[9]Yamamoto, N., Komurasaki, K. and Arakawa, Y., "Discharge Current Oscillation in Hall Thrusters," *Journal of Propulsion and Power*, Vol. 21, No. 5, 2005, pp. 870-876.

[10]Tahara, H., Goto, D., Yasui, T. and Yoshikawa, T., "Thrust Performance and Plasma Features of Low-Power Hall-Effect Thrusters," *Vacuum*, Vol. 65, No.3-4, 2002, pp.367-374.

[11]Boyd, I. D., "Review of Hall Thruster Plume Modeling," *Journal of Spacecraft and Rockets*, Vol. 38, No. 3, 2001, pp.381-387.

[12]King, L. B., Gallimore, A. D., and Marrese, C. M., "Transport-Property Measurements in the Plume of an SPT-100 Hall Thruster," *Journal of Propulsion and Power*, Vol. 14, No. 3, 1998, pp.327-335.

[13]Tajmar, M., Gonzalez, J., and Hilgers, A., "Modeling of spacecraft-Environment Interactions on SMART-1," *Journal of Spacecraft and Rockets*, Vol. 38, No. 3, 2001, pp.393-399.

[14]Ozaki, T., Inanaga, Y., Nakagawa, T., Kasai, Y., and Matsui, K., "Development status of high power xenon hall thruster of MELCO," 25th International Symposium on Space Technology and Science, ISTS 2006-b-34, 2006.

[15]King, L. B., and Gallimore, A. D., "Ion-Energy Diagnostics in the Plasma Exhaust Plume of a Hall Thruster," *Journal of Propulsion and Power*, Vol. 16, No. 5, 2000, pp.916-922.

[16]King, L. B., and Gallimore, A. D., "Mass Spectral Measurements in the Plume of an SPT-100 Hall Thruster," *Journal of Propulsion and Power*, Vol. 16, No. 6, 2000, pp.1086-1092.

[17]Gulczinski, III, F. S., and Gallimore, A. D., "Near-Field Ion Energy and Species Measurements of a 5-kW Hall Thruster," *Journal of Propulsion and Power*, Vol. 17, No. 2, 2001, pp.418-427.

[18]Gallimore, A. D., "Near- and Far-Field Characterization of Stationary Plasma Thruster Plumes," *Journal of Spacecraft and Rockets*, Vol. 38, No. 3, 2001, pp.441-453.

[19]Kim, S. W., and Gallimore, A. D., "Plume Study of a 1.35-kW SPT-100 Using an ExB Probe," *Journal of Spacecraft and Rockets*, Vol. 39, No. 6, 2002, pp.904-909.

[20]King, L., B., and Gallimore, A. D., "Ion-Energy Diagnostics in an SPT-100 Plume from Thrust Axis to Backflow," *Journal of Propulsion and Power*, Vol. 20, No. 2, 2004, pp.228-242.

[21]Gonzalez, J., and Estublier, D., "Spacecraft/thrusters interaction analysis for SMART-1," International Electric Propulsion Conference, IECP-2005-003, 2005.

[22]Taccogna, F., Longo, S., and Capitelli, M., "Particle-in-Cel with Monte Carlo Simulation of SPT-100 Exhaust Plumes," *Journal of Spacecraft and Rockets*, Vol. 39, No. 3, 2002, pp.409-419.
[23]Oh, D. Y., Hastings, D. E., Marrese, C. M., Haas, J. M., and Gallimore, A. D., "Modeling of Stationary Plasma Thruster Plumes and Implications for Satellite Design," *Journal of Propulsion and Power*, Vol. 15, No. 2, 1999, pp.345-357.
[24]Boyd, I. D., Van Gilder, D. B., and Liu, X., "Monte Carlo Simulation of Neutral Xenon Flows in Electric Propulsion Devices" *Journal of Propulsion and Power*, Vol. 14, No. 6, 1998, pp.1009-1015.
[25]Mikellides, I. G., Jongeward, G. A., Katz, I. and Manzela, D. H., "Plume Modeling of Stationary Plasma Thrusters and Interactions with the Express-A Spacecraft," *Journal of Spacecraft and Rockets*, Vol. 39, No. 6, 2002, pp.894-903.
[26]Matsui, M., Komurasaki, K., and Arakawa, Y., "Laser Absorption Spectroscopy in High Enthalpy Flows," AIAA Paper 05-5325, 2005.
[27]Demtroeder, W., Laser Spectroscopy, 3rd edition, Springer-Verlag, Berlin, 2002.
[28]Deutch, M., "Abel inversion with a simple analytic representation for experimental data," *Applied Physics Letters*, Vol 42, 1983, pp 237-239.
[29]NIST Atomic Spectra Database: http://physics.nist.gov/cgi-bin/AtData/main_asd
[30]Herzberg, G. H., Atomic Spectra and Atomic Structure, DOVER PUBLICATIONS, New York, 1945.
[31]Matsui, M., Yokota, S., Takayanagi, H., Koizumi, H., Komurasaki, K. and Arakawa, Y., "Plume Characterization of Plasma Thrusters using Diode Laser Absorption Spectroscopy," AIAA Paper 06-0767, Reno, 2006.
[32]Cedolin, J. R., Hanson, R. K., and Cappelli, M. A., "Semiconductor Laser Diagnostics for Xenon Plasmas," AIAA Paper 94-2739, 1994.
[33]Pfrommer, T., Auweter-Kurtz, M., and Winter, M. W., "Fabry-Perot Interferometry on Xenon for Future Application with Radio-frequency Ion Thrusters (RIT)," Space Technology Education Conference STEC2005, 2005
[34]Mazouffre, S., Pagnon, D., Lasgorceix, P., and Touzeau, M., "Temperature of xenon atoms in a stationary plasma thruster," International Electric Propulsion Conference, IECP-2003, 2003.